Nanoscale

Accepted Manuscript

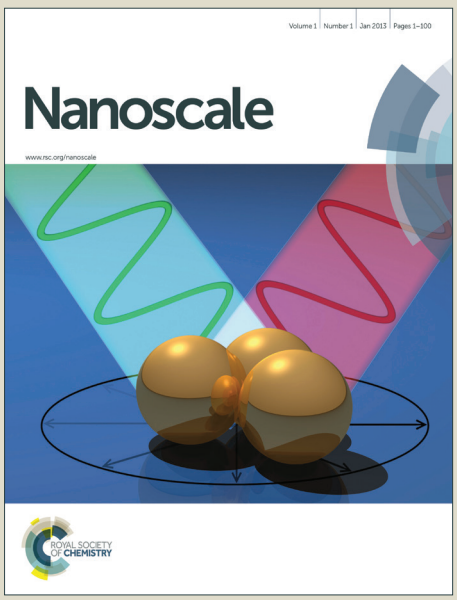

ROYAL SOCIETY OF CHEMISTRY

www.rsc.org/nanoscale

Cite this: DOI: 10.1039/c0xx00000x

www.rsc.org/xxxxxx

ARTICLE TYPE

Surface enhanced anti-Stokes one-photon luminescence from single gold nanorods

Yingbo He,[1] Keyu Xia,[2,*] Guowei Lu,[1,*] Hongming Shen,[1] Yuqing Cheng,[1] Yong-chun Liu,[1] Kebin Shi,[1,3] Yun-Feng Xiao,[1,3] and Qihuang Gong[1,3]

Received (in XXX, XXX) Xth XXXXXXXXX 200X, Accepted Xth XXXXXXXXX 200X
DOI: 10.1039/b000000x

Anti-Stokes one-photon luminescence from a single gold nanorod was investigated experimentally. The anti-Stokes emission of the gold nanorods is enhanced and modulated strongly by the localized surface plasmon resonance (LSPR). It is found that the polarization dependence of the anti-Stokes emission is in strong correlation with that of the Stokes emission. Further experiments provide evidence that the LSPR greatly enhanced both excitation and emission processes. Additionally, the line shape of anti-Stokes emission is dependent on the surface temperature which is related to the free electrons distribution near Fermi level. This discovery provides an effective way in principle to probe localized temperature at nanoscale dimension. The reported results here about the anti-Stokes emission provide more understanding for the photoemission process from the plasmonic nanostructures.

Introduction

Photoluminescence (PL) from smooth metal films was first reported with quite low quantum yield (QY) [1]. Later, PL from metallic nanostructures has been observed with much higher QY in comparison with the bulk material [2-4]. The light emission process is strongly related to the localized surface plasmon resonance (LSPR) of metallic nanostructures [2-7]. Recently, PL phenomena has received an increased interest for its potential applications in many fields, such as bright photostable label, biological molecules recognition and orientation sensing, plasmonic modes characterizing, and optical recording, etc [8-14]. Meanwhile, the anti-Stokes light emission from metallic nanostructures, of which the emitted photons have a higher energy than the absorbed photons, were usually investigated with pulsed light sources, such as two-photon luminescence [8-10,15-19]. Unlike the two-photon luminescence, the anti-Stokes one-photon luminescence receives much less attention and has only been studied in a few publication. Using a cw laser excitation, previous reports have observed the anti-Stokes one-photon luminescence from ensemble gold nanoparticles and nanorods in solution [20, 21], and from gold rough thin films [22]. Nevertheless, systematic investigation and understanding of such anti-Stokes one-photon luminescence from a single individual plasmonic nanoparticle are lacking.

Up to now, previous studies on one-photon luminescence from single plasmonic nanostructures mostly concentrated on the Stokes emission [11-13, 23-26]. In this study, we demonstrated that the Stokes emission from a single gold nanorod was always accompanied with a plasmonic surface enhanced anti-Stokes emission. In contrast to previous ensemble measurements [20-21], the anti-Stokes one-photon luminescence at single nanoparticle level provides us more knowledge about its origin. It was found that both of the anti-Stokes emission and the Stokes emission were polarization dependent and were modulated significantly by the LSPR of the gold nanorods. It indicates that both processes are coherent. Moreover, the line shape of the anti-Stokes emission was strongly modulated by the thermalized electrons distribution near the Fermi level. This finding provides a way to optically probe nanoscale localized temperature of a nanoparticle. Further experiments tuning the resonance frequency of the same particle through either photo-thermal reshaping or changing environmental index, have evidenced that the LSPR considerably enhances both excitation and emission processes and remarkably increases the anti-Stokes emission intensity.

Experiments and discussion

A single particle microspectroscopy system based on scanning probe microscope (NTEGRA Spectra, NT-MDT, Russia) was developed to combine the white light dark-field scattering, photoluminescence spectroscopy, and atomic force microscopy (AFM) techniques. The optical setup allows us to perform an *in situ* measurement to obtain the scattering and PL spectra of the same single nanoparticle. The setup has been described in detail in our previous reports [11-13]. In brief, the scattering spectra of nanoparticles were measured using a white light total internal reflection scattering method based on a high numerical aperture oil-immersion objective lens (NA 1.49, 60×TIRF, Olympus, Japan). A collimated white light beam was approximately

focused at the objective's back focal plane, and the scattering signal was collected by the same objective lens and directed into a spectrometer with a cooled CCD (iDdus, Andor). Meanwhile, the microspectroscopy system can switch easily to PL spectrum measurement excited by a cw laser at λ= 632.8 nm *in situ* for the same nanoparticle.

The gold nanorods investigated here were synthesized chemically [27,28], and the inset in Fig. 1(a) shows a representative TEM image of the synthesized nanorods. The nanorods have short axes of 20-30 nm and longitudinal axes of 50-80 nm. The nanorods were immobilized onto a glass coverslip with an average interparticle spacing of several micrometers for single particle spectroscopy measurements.

To obtain one-photon luminescence, a cw He-Ne laser at wavelength 632.8 nm (photon energy ~ 1.96 eV) was used to excite the nanorods. Meanwhile Notch filters (NF03-633E, Semrock) were utilized to obtain the Stokes and anti-Stokes emission simultaneously. The scattering spectra were recorded *in situ* with dark field white light total internal reflection technique. All spectra were measured at room temperature. The spectral shape of Stokes PL resembles roughly the scattering ones. The results agree well with previous reports for plasmonic nanostructures with simple geometrical shape [11-13, 23, 24].

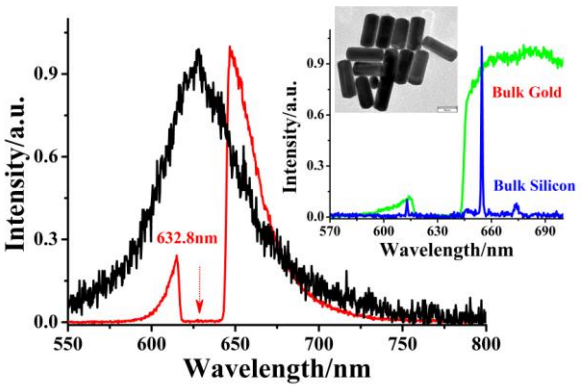

Fig. 1. Normalized scattering (black line) and PL spectra (red) of a representative gold nanorod. The inset presents the typical TEM image of the synthesized nanorods, and the emission spectra of bulk gold (green) and silicon wafer (blue) for comparison.

Interestingly, a bright anti-Stokes emission always accompanied the conventional Stokes emission when the nanorods were excited by the 632.8 nm laser. A representative spectrum (containing both Stokes and anti-Stokes components) of one-photon luminescence from a single gold nanorod is shown Fig. 1. After comparing the spectra of many single individual nanorods, it was found that the anti-Stokes emission intensity was enhanced significantly if the nanorod longitudinal LSPR matched rather than detuned away from the excitation laser frequency. To confirm the anti-Stokes signal, bulk silicon wafer and bulk gold (a magnetron sputtering target with smooth surface) were tested at the same experimental condition except for longer exposure time. The corresponding data are shown in the inset of Fig. 1. The background of the silicon spectra is low as expected. The three peaks can be ascribed to 1st Stokes and anti-Stoke, and 2nd Stokes Raman scattering, respectively. The bulk gold presents not only the Stokes signal as in previous reports but also an obvious broadband anti-Stokes emission. These observations show that the anti-Stokes emission of the gold material are truly from the intrinsic optical property of the gold material itself. By counting the excitation focus volume and original spectral intensity roughly, the anti-Stokes emission brightness per gold atom of the nanorod is over 3 orders of magnitude higher than that of the bulk material.

The anti-Stokes one-photon luminescence of gold nanostructures has been reported in previous studies, but the properties were not investigated and discussed in detail [20-22]. For instance, anti-Stokes emission from an ensemble of 25 nm diameter gold nanoparticles in solution was observed in Ref. [20]. The authors claimed that the spectral shape of one-photon luminescence was similar to the absorption spectrum [20]. Very recently, the study on an ensemble of gold nanorods in solution showed that the anti-Stokes spectrum can be well fitted by a thermal population of excitations [21]. Also, an obvious anti-Stokes emission was detected from a rough gold film illuminated by a cw 780 nm laser [22]. Here, the anti-Stokes one-photon luminescence was studied at a single individual gold nanorod level. The dependence on the excitation power and polarization, and the collection polarization were systematically investigated.

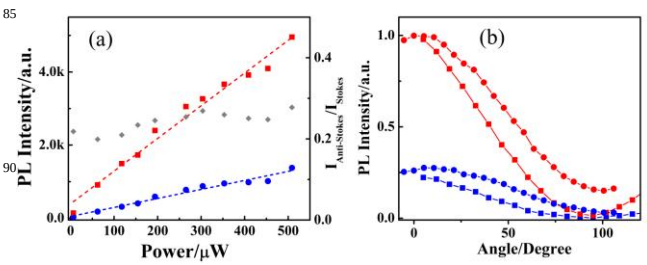

Fig. 2. Dependences of the PL intensity of a single nanorod on excitation laser power (a) and polarization (b). In (a), the Stokes (red squares) and anti-Stokes (blue circles) emission intensities increase linearly as the excitation power increasing; the ratio of Stokes emission intensity to anti-Stokes one remains a constant almost. The dashed lines are fitted curves. In (b), the Stokes (red) and anti-Stokes (blue) emission intensity present a correlated polarization dependence on the excitation polarization (squares) and collection polarization (circles).

The dependences of the PL intensity on the excitation laser power and polarization are shown in Fig. 2. Both of the Stokes and anti-Stokes emission have approximately linear laser-power dependence. It indicates a *linear* one-photon excitation process [see Fig. 2(a)]. Instead, the ratio of the integrated Stokes emission intensity to the anti-Stoke one remains constant as the excitation power was increased. By using a $\lambda/2$ wave plate to tune the angle between excitation light polarization and the longitudinal axis of the nanorod, as seen from Fig. 2(b), the polarization dependence was observed. For the first time, we observed that the anti-Stokes emission is in strong correlation with the Stokes emission in polarization, and follow $\cos^2\theta$ dependence as the Stokes emission [12, 23]. Both the anti-Stokes and Stokes emission intensity varied as the excitation polarization being

rotated, and reached a maximum when the polarization of the excitation was parallel along the nanorod longitudinal axis. Additionally, the collection polarization dependence of the Stokes and anti-Stokes emission were also investigated. Again, the anti-Stokes emission behaves similarly as the Stokes emission, and the polarization of PL from the nanorod was always parallel to the longitudinal axes as an electric dipole radiation. This strong correlation means that both anti-Stokes and Stokes emissions share a common process and this process cannot be ascribed simply to a pure thermal emission as stated previously [15]. All the results imply that both Stokes and anti-Stokes emission are resulted from the same physical origin, i.e. it should be strongly related to the LSPR of the gold nanorods.

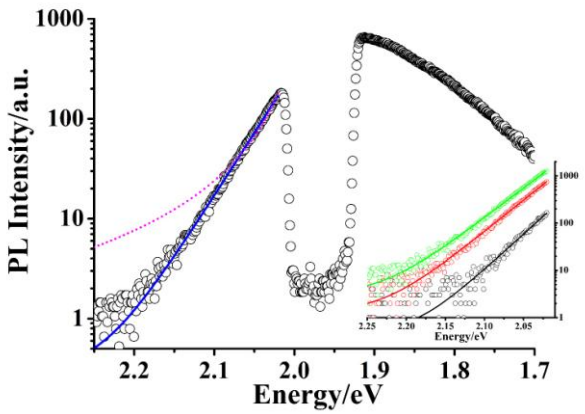

Fig. 3. Anti-Stokes emission as a function of photon energy. The data is fitted (lines) by Boltzmann statistics distribution (blue solid line) and Lorentz line shape (purple dashed line) for the anti-Stokes part, respectively. The inset presents anti-Stokes spectra at different illumination light intensities and corresponding fitting lines with Boltzmann statistics.

The spectral profile of the anti-Stokes emission is another interesting topic. As shown in Fig.3, the intensity of anti-Stokes emission decays exponentially, to a good approximation, as photon energy was increased, which is consistent with a recent report of ensemble gold nanorods in solution, i.e. the line shape can be described by a thermal population of excitations [21]. This exponential decay behavior probably attributes to the distribution of thermalized electrons near the Fermi level. Generally, the *sp*-band free electrons can respond to optical radiation directly and decay rapidly due to the electron-electron and electron-phonon thermalization processes, which have been investigated using femtosecond pump-probe techniques [29-32]. In the present study, the electrons and lattice should reach quasi thermal equilibrium under the cw laser illumination, due to large electron population, high rate of electron-electron, and electron phonon processes [2,30,31]. The electrons occupation in *sp*-band near Fermi level follows the Fermi-Dirac distribution, i.e. $\propto (1 + e^{\Delta E / K_B T})^{-1}$. Here, the distribution can be simplified to follow Boltzmann statistic distribution $\propto e^{-\Delta E / K_B T}$ approximately at room temperature [21, 25, 29-32]. Therefore, the line-shape of anti-Stokes emission is dominated by the thermal equilibrium electron distribution, meanwhile the emission rate is also enhanced greatly by the nanorod LSPR. As seen from Fig. 3, the anti-Stokes emission as a function of the photon energy can be fitted well with Boltzmann statistics, but not Lorentzian which is often effective for the Stokes emission.

Furthermore, measuring the anti-Stokes spectrum provides us a way to probe the localized temperature at nanoscale. This nanoscale temperature optical sensing promises potential applications in many fields such as nanoscale biological temperature sensing. In the present case, the surface temperature of the nanorod under different illumination power can be extracted through fitting the anti-Stokes emission, as shown in Fig. 3 and [32]. For instance, ΔT (above room temperature) of about 65 $\pm$ 5 K, 126$\pm$3 K, and 160 $\pm$2 K for excitation power 100 μ W, 300 μ W, and 500 μ W can be determined, respectively. The nanorod photothermal reshaping was found at $\Delta T \approx 180^{\circ}C$ which is consistent with previous results [24]. Note that the threshold temperature of photothermal reshaping for each individual nanoparticle varies from sample to sample due to the dispersion in size and shape, etc. Therefore, anti-Stokes emission from a single gold nanorod can provide an effective way in principle to sense a nanoscale localized temperature by fitting the anti-Stokes spectrum. Further efforts to demonstrate the ability of nanoscale thermometer is under way by adjusting the environmental temperature.

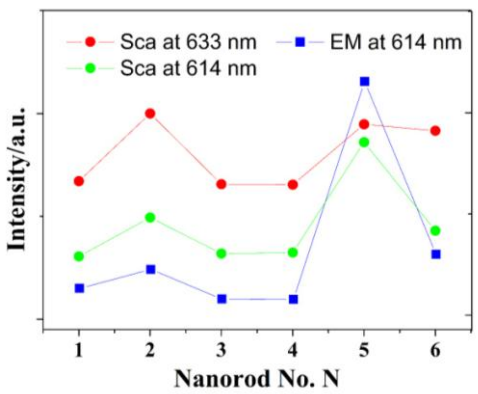

Fig. 4. Anti-Stokes emission intensities at wavelength of 614 nm (blue), and the relative scattering intensity at wavelength of 633 nm (red) and 614 nm (green) for 6 different individual nanorods excited by 633 nm laser, respectively.

Furthermore, the experimental observation of anti-Stokes emission provides a good way to understand the PL process because of the low background at the anti-Stokes side. Up to now, it is widely accepted that the LSPRs play an important role in the photoemission process of metallic nanostructures although there is not an undisputed model for the process [7, 24, 33, 34]. Two probable mechanisms (i) plasmon-enhanced interband transitions of *d*-band electrons into *sp*-band and subsequent radiative recombination; (ii) the excited *d*-band holes recombine nonradiatively with *sp*-band electrons, then emitting particle plasmon which subsequently radiate, have been proposed to explain the light emission [7, 21, 22, 24, 33, 34]. The above two models based on *e-h* pair recombination scheme consider the excitation and emission process modified by the surface plasmon respectively.

According to the experimental measurement of anti-Stokes emission, it is evidenced that the LSPRs of plasmonic nanostructures not only influence the excitation rate but also modify the emission efficiency. In this study, the *sp*-band free electrons dominate the light emission process. The photon energy at wavelength 632.8 nm (or 780 nm in previous reports) is assumed to be unable to excite the *d*-band electrons efficiently (although the interband transition at X-point could involve) [23]. While the laser can couple with or excite directly the *sp*-band free electrons. Meanwhile the *sp*-band free electrons are also related strongly to LSPRs due to electron collective oscillations. As seen from Fig. 1, the one-photon luminescence of the nanorods is in strong correlation with the scattering spectrum. Thus, the excitation and emission processes are modulated by the LSPRs strongly. More convincing evidences are demonstrated by correlating the original data of the scattering spectra and the PL spectra from different single nanorods. As shown in Fig. 4, the anti-Stokes PL intensity at wavelength 614 nm from different shapes of nanorods follows the trend of the scattering intensities at excitation (at 633 nm), emission (at 614 nm), and their products. Clearly, the anti-Stokes emission is correlated with the scattering. In present study, the single nanorods being investigated had a narrow distribution of their size and aspect ratio. The scattering and absorption cross-section can be considered approximately to vary linearly in the same trend in a narrow range [35]. Then, the scattering intensity at 633 nm is approximately related to the absorption cross section of the nanorods. For emission process, the scattering intensity at 614 nm can be assumed to be proportional to the radiative rate of plasmon emission [36]. As a result, the relative anti-Stokes emission intensity of different individual nanorods can be estimated roughly and then can be compared with the scattering intensities at the excitation and emission wavelengths. The experimental observations indicated clearly that the LSPRs can enhance both the photon absorption and emission process during the photo emission.

To demonstrate the influence of nanorod LSPRs on the light emission, we adjusted the LSPR peak position of the same isolated nanoparticle, and measured the PL and scattering spectra *in situ*. The LSPRs peak of the nanorods were changed towards longer wavelength by increasing their environmental medium index, or can be tuned towards shorter wavelength by photothermal reshaping effects [11, 12, 24]. At first, the scattering and PL spectra of single nanorod were collected in air, then measured *in situ* after immersing it in water as shown in Fig. 5a. It can be clearly seen that the anti-Stokes emission decreases dramatically as the LSPRs are red-shift. The ratio of anti-Stokes emission intensity to Stokes also decreases considerably due to less absorption and lower emission enhancement caused by the LSPR. In addition, the laser heating effect was applied to induce shape transformation of a nanorod towards a spherical shape. This reshaping results in the blue-shift of LSPRs. As seen from Fig. 5b, the scattering peak of the nanoparticle blue-shifts gradually but the intensity remains similar during the transformation of the nanorod to a sphere-like shape. It confirms that the volume of the particles is maintained. Thus, the absorption cross-section remains almost the same at the resonant frequency, but changed at excitation wavelength because the LSPR peak shifted away from the excitation wavelength. In contrast, the intensity of PL decreases quickly as photothermal reshaping due to the shape dependence of the quantum efficiency of the light emission. Our measurements were in good agreement with previous report that the QY decreases when the nanorod becomes a spherical nanoparticle [24]. Although the absolute intensity of anti-Stokes emission decreases slightly at last, the ratio of anti-Stokes to Stokes emission intensity increased greatly after the shape transformation because the Stokes emission decreases dramatically. In the end, the anti-Stokes emission efficiency becomes comparable to that of the Stokes emission because the LSPR peak overlaps well with the anti-Stokes emission band. All results obviously verify that the LSPR influences both the excitation and emission processes during the photoemission from the plasmonic nanostructures.

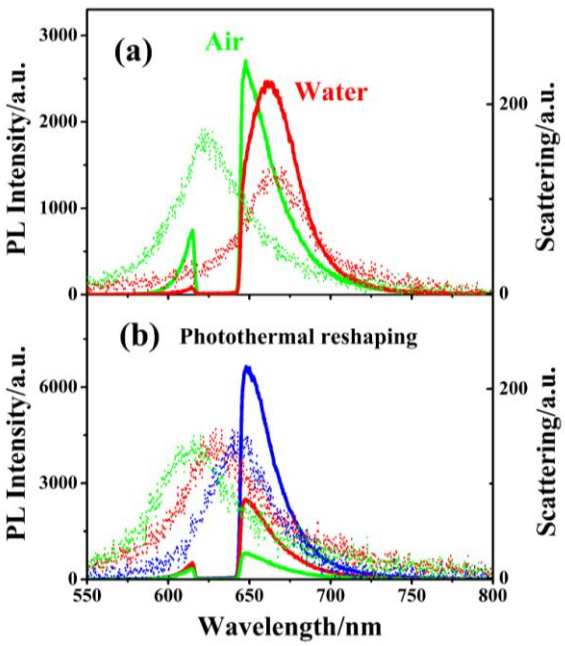

Fig. 5. Light emission spectra as the local surface plasmon resonance frequencies being changed. (a) The scattering (dots) and PL (solids lines) spectra of the same nanorod in air (green) and water (red). (b) The scattering (dots) and PL (solids) spectra of a single individual nanoparticle reshaped through photothermal effect. All spectra were recorded after photothermal reshaping with the same excitation intensity.

So far, there is not an undisputed model yet for the photoemission process of metallic nanostructures although it is widely accepted that the LSPR play an important role in the process [2, 7, 15, 22, 26, 33, 34]. Generally, in metallic nanostructures like gold nanorods, the *sp*-band free electrons can interact with photons directly. In other word, it can be driven by a laser to oscillate collectively. Such collective oscillation of free electrons (COFE) in a metallic nanoparticle can emit photons radiatively as plasmon emission [23, 34]. In order to understand both the Stokes and anti-Stokes emission, we propose a theoretical model by treating a single gold nanorod as a

plasmonic resonator supporting a quantized COFE. On the basis of the concept of the optical cavity, we model the PL of the single gold nanorod as the radiative emission of COFE from the nanorod's LSPR mode. Our model involves four processes: (i) the laser drives the COFE; (ii) the created COFE excites the LSPR mode as the input; (iii) the LSPR mode generates an output out of the COFE surrounding the surface of the nanorod; (iv) the mode-generated COFE couples to the light and generates the photon emission. The detail description of the theoretical model is well-documented elsewhere [32].

Specifically, the coupling efficiency between the light and the COFE is proportional with the spatial and temporal overlap of the modes. Additionally, when a cw laser beam illuminates on the gold nanorod, the *sp*-band free electrons gaining energy and then rapidly reaches its thermal equilibrium due to the fast electron-electron and electron-phonon interaction [30,31]. Then, the collective oscillation of free electrons involved in LSPR mode is modulated by the free-electron state density. In the thermal equilibrium, the electron state density often follows the Fermi-Dirac statistic distribution [2, 30]. Therefore, the light emission process is related to both the *sp*-band free-electron distribution and the localized surface plasmon resonance. Approximately, the distribution of free electron state density under Fermi level for *sp*-band electrons, which modulates the Stokes emission as well, is flat as function of photon energy. Therefore, the spectral line shape which is dominated by the LSPR mode, takes the Lorentzian profile. In contrast, for the anti-Stokes emission, the electrons near or up Fermi level is approximately a Boltzmann distribution, (the emission rate is enhanced in the same way by the surface plasmon). Then, the line shape of anti-Stokes emission is governed by the Boltzmann distribution. Our theory explains qualitatively the difference between spectral line shapes of Stokes and anti-Stokes one-photon luminescence from single gold nanorods [32]. It also provides an understanding for the relation between the anti-Stokes spectral line shape and the surface temperature of gold nanorods. The theoretical model provides a self-consistent and unified understanding for both the anti-Stokes and Stokes one-photon luminescence from noble metal nanoparticles.

Conclusions

To summarize, we have investigated experimentally the one-photon luminescence from a single gold nanorod in detail. Besides the conventional Stokes emission, a bright anti-Stokes emission has been observed clearly. It is enhanced by the LSPR of the plasmonic nanostructure. By using a low photon energy to excite the single gold nanorod, the anti-Stokes process avoids the influence of background signal due to interband transition. It was found that both plasmon enhanced excitation and plasmon emission contribute to the photoluminescence process of the metallic nanostructures. Additionally, the anti-Stokes component is also modulated by the free electron distribution near the Fermi level, which can be used to extract localized temperature information of a single nanoparticle. A new theoretical model was applied to explain qualitatively spectral line shape of one-photon luminescence from gold nanorods.

This work was supported by the National Key Basic Research Program of China (grant nos.2013CB328703) and the National Natural Science Foundation of China (grant nos. 61422502, 11374026, 91221304, 11121091).

Notes and references

[1]*State Key Laboratory for Mesoscopic Physics, Department of Physics, Peking University, Beijing 100871, China*
[2]*ARC Centre for Engineered Quantum Systems, Department of Physics and Astronomy, Macquarie University, NSW 2109, Australia*
[3]*Collaborative Innovation Center of Quantum Matter, Beijing 100871, China*
E-mail: guowei.lu@pku.edu.cn; xiakeyu@gmail.com

[1] A. Mooradian, Phys. Rev. Lett. 22, 185 (1969).

[2] F. T. Boyd, Z. H. Yu, and Y. R. Shen, Phys. Rev. B 33, 7923 (1986).

[3] M. B. Mohamed, V. Volkov, S. Link, and M. A. El-Sayed, Chem. Phys. Lett. 317, 517 (2000).

[4] X. Wu, T. Ming, X. Wang, P. Wang, J. Wang, and J. Chen, ACS Nano 4, 113 (2010).

[5] N. Yamamoto, K. Araya, and F. J. G. de Abajo, Phys. Rev. B 64, 205419 (2001).

[6]P. Biagioni,J.-S. Huang, and B. Hecht, Rep. Prog. Phys. 75, 024402 (2012).

[7] O. P. Varnavski, T. G. III, M. B. Mohamed, and M. A. El-Sayed, Phys. Rev. B 72, 235405 (2005);

[8] H. Wang, T. B. Hu, D. A. Zweifel, W. H, P. S. Low, A. Wei, and J. Cheng, Proc. Nat. Acad. Sci. U. S. A. 102, 15752 (2005).

[9] R. A. Farrer, F. L. Butterfield, V.W. Chen, and J. T. Fourkas, Nano Lett. 5, 1139 (2005).

[10] N. J. Durr, T. Larson, D. K. Smith, B. A. Korgel, K. Sokolov,and A. Ben-Yakar, Nano Lett. 7, 941 (2007).

[11] G. Lu, L. Hou, T. Zhang, J. Liu, H. Shen, C. Luo, and Q. Gong, J. Phys. Chem. C 116, 25509 (2012).

[12] T. Zhang, H. Shen, G. Lu, J. Liu, Y. He, Y. Wan, and Q. Gong, Adv. Optical Mater 1, 335(2013).

[13] T. Zhang, G. Lu, H. Shen, K. Shi, Y. Jiang, D. Xu, and Q. Gong, Sci. Rep. 4, 3867 (2014).

[14] P. Zijlstra, J. W. M. Chon, and M. Gu, Nature 459, 410 (2009).

[15] M. B. Agranat, A. A. Benditskii, G. M. Gandelman, A. G. Devyatkov, P. S. Kondratenko, B. I. Makshantsev, G. I. Rkman, and B. M. Stepanov, JETP Lett. 30,167(1979).

[16]M. D. Wissert, K. S. Ilin, M. Siegel, U. Lemmer,and H.-J. Eisler, Nano Lett. 10, 4161 (2010).

[17]K. Imura and H. Okamoto, J. Phys. Chem. C 113, 11756 (2009).

[18]E. J. R. Vesseur, R. de Waele, M. Kuttge, and A. Polman, Nano Lett. 7, 2843 (2007).

[19]A. Bouhelier, R. Bachelot,G. Lerondel, S. Kostcheev, P. Royer, and G. P. Wiederrecht, Phys. Rev. Lett. 95, 267405 (2005).

[20] Y. N. Hwang, D. H. Jeong, H. J. Shin, D. Kim, S. C. Jeoung, S. H. Han, J. S Lee, and J. Cho, J. Phys. Chem. B 106, 7581 (2002).

[21] J. Huang, W. Wang, C. J. Murphy, and D. G. Cahill, Proc. Nat. Acad. Sci. U. S. A. 111, 906 (2014).

[22] M. R. Beversluis, A. Bouhelier, and L. Novotny, Phys. Rev. B 68, 115433 (2003).

[23] A. Tcherniak, S. Dominguez-Medina, W. Chang, P. Swanglap, L. S. Slaughter, C. F. Landes, and S. Link, J. Phys. Chem. C 115, 15938 (2011).

[24] M. Yorulmaz, S. Khatua, P. Zijlstra, A. Gaiduk, and M. Orrit, Nano Lett. 12, 4385 (2012).

[25] H. Hu, H. Duan, J. K. W. Yang, and Z. X. Shen, ACS Nano 6,10147 (2012).

[26]Y. Fang, W.-S. Chang, B. Willingham, P. Swanglap, S. Dominguez-Medina, and S. Link, ACS Nano 6, 7177 (2012).

[27] B. D. Busbee, S. O. Obare, C. J. Murphy, Adv. Mater. 15, 414−416 (2003).

[28] H. Chen, L. Shao, K. C. Woo, T. Ming, H. Lin, and J. Wang, .J. Phys. Chem. C 113,17691–17697 (2009).

[29] G. Sauerbre, E.Woeckel, and P. Dobberstein, Phys. Stat. Sol. (b) 60, 665 (1973).

[30] J. Hohlfeld, S. S. Wellersho_, J. Gudde, U. Conrad, V. Jahnke, and E. Matthias, Chem. Phys. 251, 237 (2000).

[31] C. K. Sun, F. Vallee, L. H. Acioli, E. P. Ippen, and J. G. Fujimoto, Phys. Rev. B 50, 15337 (1994).

[32] K. Xia, Y. He, G. Lin, H. Shen, Y. Cheng, Q. Gong, G. Lu, arXiv:1407.6105.

[33] T. V. Shahbazyan, Nano Lett. 13, 194 (2013).

[34] E. Dulkeith, T. Niedereichholz, T. A. Klar, J. Feldmann, G. von Plessen, D. I. Gittins, K. S. Mayya, and F. Caruso, Phys. Rev. B 70, 205424 (2004).

[35] W. Ni, X. Kou, Z.Yang, and J. Wang, ACS Nano 2, 677-686 (2008).

[36]U. Kreibig and M. Vollmer, Optical Properties of Metal Clusters (Springer, New York, 1995).